Michigan State University

National Superconducting Cyclotron Laboratory

COLLECTIVE EXPANSION IN CENTRAL Au + Au COLLISIONS

W.C. HSI, G.J. KUNDE, J. POCHODZALLA, W.G. LYNCH, M.B. TSANG, M.L. BEGEMANN-BLAICH, D.R. BOWMAN, R.J. CHARITY, A COSMO, A. FERRERO, C.K. GELBKE, T. GLASMACHER, T. HOFFMANN, J. HUBELE, G. IMME, I. IORI, J. KEMPTER, P. KREUTZ, W.D. KUNZE, V. LINDENSTRUTH, M.A. LISA, U. LYNEN, M. MANG, A. MORONI, W.F.J. MÜLLER, M. NEUMANN, B. OCKER, C.A. OGILVIE, G.F. PEASLEE, G. RACITI, F. ROSENBERGER, H. SANN, R. SCARAONI, A. SCHÜTTAUF, C. SCHWARZ, W. SEIDEL, V. SERFLING, L.G. SOBOTKA, L. STUTTGE, W. TRAUTMANN, A. TUCHOLSKI, C. WILLIAMS, A. WÖRNER and B. ZWIEGLINSKI

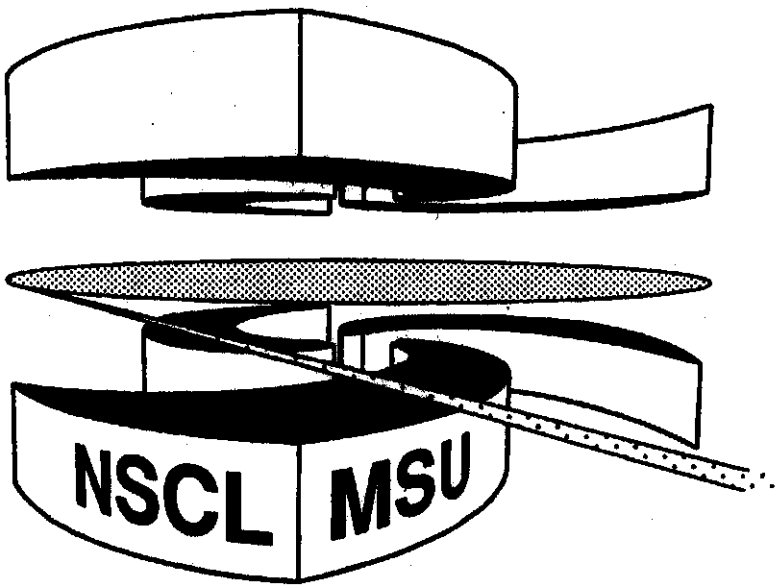

MSUCL-930

MAY 1994

Collective Expansion in Central Au+Au Collisions

W.C. Hsi[a], G.J. Kunde[b], J. Pochodzalla [b], W.G. Lynch", M.B. Tsang[a], M.L. Begemann-Blaich[d], D.R. Bowman[a,1], R. J. Charity[c], A. Cosmoe, A. Ferrero[f,2], C.K. Gelbke[a], T. Glasmacher[a], T. Hofmann[b], J. Hubele[b], G. Imme[g], I. Iori[f], J. Kempter[d], P. Kreutz[d], W.D. Kunze[b], V. Lindenstruth[b], M.A. Lisa[a,3], U. Lynen[b], M. Mang[d], A. Moroni[f], W.F.J. Müller[b], M. Neumann[d], B. Ocker[d], C.A. Ogilvie[b,4], G.F. Peaslee[a, 5] G. Raciti[g], F. Rosenbergerd, H. Sann[b], R. Scardaoni[f], A. Schüttauf[d], C. Schwarz[a], W. Seidel[h], V. Serfling[d], L.G. Sobotkac, L. Stuttge[e], W. Trautmann[b], A. Tucholski[i], C. Williams[a], A. Wörner[b], and B. Zwieglinski[i]

[a]*Department* of *Physics and Astronomy and National Superconducting Cyclotron Laboratory ,Mickigan* State *University, East Lansing, MI 48824, USA;* [b]*Gesellschaft für Sckwerionenforsckung, D-64220,Darmstadt, Germany;* [c]*Department* of *Chemistry, Washington University, St. Louis, MO 63130, USA;* [d]*Institut für Kernphysik, Universitat Frankfurt, 60486 Frankfurt, Germany;* [e]*Centre de Reckerckes Nucléaires, Strasbourg, France;* [f]*I.N.F.N. and Dipartimento di Fisica, Università degli Studi di Milano, l-20133 Milano, Italy;* [g]*I.N.F.N. and Dipartimento di Fisica dell' Università, I-95129 Catania, Italy;* [h]*FZ Rossendorf, DO1314 Dresden, Germany;* [i]*Soltan Institute* for *Nuclear Studies, Hoza 69, 00-681 Warsaw, Poland.*

Abstract

Energy spectra for intermediate mass fragments produced in central Au+Au collisions at E/A=100 MeV provide strong evidence for a collective expansion at breakup. Values ranging over $E_r/A \approx$ 8.3-12.5 MeV, extracted for this collective expansion energy, decrease somewhat with the fragment charge, but are relatively insensitive to the breakup density, transverse collective flow and the incomplete damping of the initial longitudinal collective motion of projectile and target nucleons.

PACS numbers: 25.70.Np, 25.70.Gh

---

[1] Present Address: Chalk River Laboratories, Chalk River, Ontario KOJ 1J0, Canada;

[2] On leave from the Comision Nacional Energia Atomica, Argentina.

[3] Present Address: Lawrence Berkeley Lab, Berkeley Ca.

[4] Present Address: Department of Physics, MIT, Cambridge, MA 02139.

[5] Present Address: Physics Deparhnent, Hope College, Holland, MI.

Investigations of the incident energy dependence of central collisions between heavy nuclei reveal a rise to a maximum in the multiplicity of intermediate mass fragments (IMF's; Z_f =3-30) at $E_{beam}/A \approx 100$ MeV, followed by a decline into vaporization at higher incident energies [1,2]. Such observations are qualitatively consistent with the excitation energy dependencies of statistical models of nuclear disassembly [3-5] and interpretations which embody nuclear phase transitions [3,4,6,7]. The maximum near $E_{beam}/A \approx 100$ MeV, however, is predicted by dynamical models [8,9] to be the consequence of a rapid expansion of the nuclear system from a state of supranormal density achieved early in the nuclear collision [8].

Recent experimental evidence suggests a significant collective expansion [10-13], but little has been published to quantify the resulting collective radial flow. Most measurements have focused on flow directed sidewards, parallel to the reaction plane of the colliding system [14-16]. Such effects are large at E/A=400 MeV, but decrease and become minimal at lower incident energies near the "balance energy" [17], where the mean field attraction and the repulsive influence of nucleon-nucleon collisions become comparable. Experimental determination of flow, transverse [14-16] or radial [10,13], can provide important constraints on nuclear transport properties [18].

To investigate collective expansion in Au+Au collisions at E/A=100 MeV, thin ^{197}Au targets of 3 and 5 mg/cm^2 areal density were bombarded at the SIS facility of GSI by ^{197}Au ions of E/A= 100 and 400 MeV incident energy. Charged particles emitted to θ_{lab} = 14°-160° were detected in 215 plastic scintillator - CsI(Tl) phoswich detectors of the Miniball/Miniwall [19]. Particles which penetrated the plastic-scintillator foils of these phoswich detectors were identified by element for Z≤10 and by isotope for Z=1 and 2. For $25° \le \theta_{lab} \le 160°$, 4 mg/cm^2 plastic scintillator foils were used, leading to energy thresholds for particle identification of $E_{th}/A \sim 1.5$ MeV (2.5 MeV) for Z=3 (Z=10) particles, respectively. For $14° \le \theta_{lab} \le 25°$, 8 mg/cm^2 plastic foils were used leading to energy thresholds of $E_{th}/A \sim 2.2$ MeV (4.5 MeV) for Z=3 (Z=10) particles,

respectively. Lower energy particles were included in the measured charged particle multiplicity N_C, but not identified. Energy calibrations, accurate to 10%, were obtained by combining the "punch through" points measured in this experiment with detailed detector response functions measured at the NSCL K1200 Cyclotron of Michigan State University [20].

Radial flow effects should be enhanced for central collisions [18] selected, for example, by charged particle multiplicity. Assuming the charged particle multiplicity decreases monotonically with impact parameter, a "reduced" impact parameter, $\hat{b} = b/b_{max}$, was determined following refs. [1,21,22]; here, b_{max} was defined by $\langle N_C(b_{max})\rangle = 4$. Laboratory energy spectra for Boron fragments emitted in near central collisions ($\hat{b} < 0.33$) are shown in Fig. 1; they display exponential slopes that become steeper with scattering angle. Such behavior is expected for symmetric systems due to their large center-of-mass (CM) velocity. Insufficient damping of the incident collective linear momenta of projectile and target due to transparency [23] or contributions from non-central collisions can result in additional elongations of the momentum distributions parallel to the beam axis. Such effects are well known, and can be well described at lower incident energies by a superposition of three isotropically emitting thermal sources corresponding to the decay of the participant region in addition to the decay of projectile- and target-like spectator nuclei [24,25].

The solid lines in the upper panel in Fig. 1 indicate bests fits to the energy spectra assuming three relativistic Maxwellian distributions [26],

$$\frac{dP(\vec{p})}{dEd\Omega} = \sum_{i=1}^{3} \frac{dP_i(\vec{p})}{dEd\Omega} = \frac{dP_1}{dEd\Omega}(\vec{p}, \vec{V}_1, V_1) + \int_0^{2\pi} \frac{d\phi_R}{2\pi} \sum_{i=2}^{3} \frac{dP_i}{dEd\Omega}\left(\vec{p}, \vec{V}_i(\phi_R), V_i\right) \qquad (1)$$

where E and $\vec{p}$ denote the kinetic energy and momentum of the emitted particle; $\vec{V}_i$ denotes the velocity and V_i the effective Coulomb barrier of the i^{th} source; ϕ_R denotes the azimuthal angle of the reaction plane [27]. Here, $\frac{dP_i}{dE\,d\Omega}(\vec{p}, 0, V_i)$ is defined in the rest frame of the source ($\vec{V}_i \equiv 0$) by

$$\frac{dP_i}{dE\,d\Omega}(\vec{p},0,V_i) = a_i \cdot \Theta\left(E-V_i\right)\left(E+mc^2-V_i\right)\sqrt{\left(E+mc^2-V_i\right)^2-m^2c^4}\,\exp\left(-\frac{E-V_i}{T_i}\right) \quad (2)$$

and $\frac{dP_i}{dE\,d\Omega}(\vec{p},\vec{V}_i,V_i)$ is obtained from Eq. 2 by Lorentz transformation. In Eq. 2, a_i is a normalization constant, T_i is the temperature of the Maxwellian source, and $\Theta\left(E-V_i\right)$ is the unit step function. The mass m was taken to be that of the most abundant natural isotope, e.g. A=11 for Boron. Because of symmetry, we required in the CM frame $\vec{V}_3 = -\vec{V}_2$, $a_3 = a_2$, and $T_3 = T_2$. The fit parameters are given in Table 1. The transverse velocity for the spectator sources (i=2,3) were determined from fits to triple differential cross sections measured with respect to the reaction plane [28]. Reasonable variations of this velocity component influence little the parameters of the participant source.

Contributions from the participant source (dashed lines) dominate the fits at θ_{lab} = 35.5° and 45°. Spectator sources contribute strongly at backward angles and for very high energies at forward angles, indicating undamped longitudinal collective motion, but they do not contribute strongly at 28° ≤ θ_{lab} ≤ 57.5° for 400 MeV ≤ E_{lab} ≤ 700 MeV. Unlike spectra measured at lower incident energies [24] or for mass asymmetric systems [25], the present spectra are very poorly described by thermal source fits at these angles and energies that are dominated by mid-rapidity emission from the participant source. Similar difficulties are encountered for the energy spectra of other IMF's with 3 ≤ Z_f ≤ 6.

The impact parameter gate, $\hat{b} < 0.33$, includes non-central collisions of large angular momentum. Thus, both "rotational" flow (due to the nuclear mean field attraction [29,30]) and repulsive transverse collective flow (due to nucleon-nucleon collisions, Coulomb interactions and the repulsive high density mean field potential [14]) can influence the momentum and energy distributions. Such effects will be reflected by a focusing of the emitted particles into [29,30] or perpendicular to [15,16] the reaction plane, and can be observed by constructing α-α azimuthal angular correlation functions, $1+R(\Delta\phi_{\alpha\alpha})$, defined by

$$\sum Y_{12}(\vec{p}_1,\vec{p}_2) = [1+R(\Delta\phi_{\alpha\alpha})]\cdot\sum Y_1(\vec{p}_1)\sum Y_2(\vec{p}_2). \quad (3)$$

Here, $Y_{12}(\vec{p}_1,\vec{p}_2)$ is the coincidence yield, $Y_1(\vec{p}_1)$ and $Y_2(\vec{p}_2)$ are the singles yields for the particles 1 and 2 at momenta $\vec{p}_1$ and $\vec{p}_2$, and $\Delta\phi_{\alpha\alpha} = \phi_{\alpha 1} - \phi_{\alpha 2}$ is the relative azimuthal angle between the two alpha particles about the beam axis. Both sides of Eq. 3 are summed over momenta $\vec{p}_1$and $\vec{p}_2$ for fixed $\Delta\phi_{\alpha\alpha}$ subject to an energy threshold of E/A > 10 MeV and common centrality and rapidity gates.

The open squares in Fig. 2 depict α-α azimuthal correlations resulting from strong sideward directed flow, for Au+Au collisions at E/A=400 MeV selected by $\hat{b} <$ 0.33 and a gate slightly below mid-rapidity at $0.25 \le y_\alpha/y_{beam} \le 0.5$. A pronounced maximum is observed at $\Delta\phi_{\alpha\alpha} \approx 0$; it results from the repulsive deflection [14] ("bounce off") of both α -particles from the participant region. In contrast, the corresponding mid-rapidity data at E/A=100 (open circles) reveal only small directed flow components and no indication of a "V" shaped correlation characteristic of the "rotational" flow pattern observed at lower incident energies [29,30]. Some directed flow components can be identified near the target rapidity (solid circles), but these do not influence spectra at θ_{lab} = 35.5° or 45°.

Thus, if transverse collective motion contributes at E/A=100 MeV near mid-rapidity, it is not strongly correlated with the reaction plane. To determine whether the descrepancy between fitted and measured spectra in the upper panel of Fig. 1 can be explained by a collective radial flow, a self similar radial expansion, $\vec{V}(\vec{r}) = c\beta_{exp}\vec{r}/R_S$, of the spherical participant source (i=1 in Eq. 1) was assumed which attains its maximum velocity $c\beta_{exp}$ at the surface r = R_S. The velocities of individual particles were assumed to be thermally distributed about the local radial expansion velocity with temperature T_1. Coulomb expansion after breakup was modeled in the limit of large β_{exp}, i.e. particles with charge Z_f, emitted from a source with charge Z_S, were aasumed to gain the kinetic energy $\Delta E_{Coul}(r) = Z_f(Z_S - Z_f)e^2r^2/R_S^3$, without changing their direction. In the CM frame one obtains

$$\frac{dP_1}{dEd\Omega} = \frac{3}{4\pi R_S^3}\int_0^{R_S} r^2 dr \int d\Omega_r \int dE' \frac{dP_1}{dE'd\Omega}\left(\vec{p}', \vec{V}(\vec{r}), 0\right)\delta\left(E' - E + \Delta E_{Coul}(r)\right), \quad (4)$$

where the direction of the particle's momentum is assumed to be unchanged. The total energy spectrum is obtained by inserting Eq. 4 into Eq.1 as the participant source.

Energy spectra for Z_f = 2 - 6 have been fitted using Eq. 4 and a non-zero radial expansion. Best fits, assuming Z_S = 118 and R_S = 10 fm, are shown by the solid lines in the lower panel of Fig. 1; they accurately follow the curvature in the energy spectra at $28° \leq \theta_{lab} \leq 57.5°$ where the participant source dominates. Extracted values for β_{exp} are not very sensitive to the spectral temperature T_1. They change by about ±10% as T_1 varies over the range 5 MeV $\leq T_1 \leq$ 20 MeV over which reasonable fits were obtained. Values of β_{exp}, extracted for different values of Z_f, are shown in the left panel of Fig. 3; they are similar when T_1 is varied freely (open points) or is held fixed (solid points) at T_1 = 15 MeV. Somewhat smaller radial expansion velocities are observed for heavier fragments. Values for β_{exp} are not significantly changed by making a more restrictive gate, $\hat{b} < 0.16$, on the impact parameter.

Since β_{exp} and the Coulomb expansion dynamics have a similar influence on the energy spectra, there is a ± 3% variation in β_{exp} with the breakup density over the interval $\rho = 0.1\text{-}0.3\rho_o$. This latter sensitivity is largely absent in the mean total radial collective energy defined by $\langle E_r \rangle = \frac{3}{5}\left(\frac{1}{2}mc^2\beta_{exp}^2 + Z_f(Z_S - Z_f)e^2R_S\right)$, shown as the solid points in the right panel of Fig. 3. A linear increase in $\langle E_r \rangle$ with mass (charge) is observed for $Z_f \leq 4$, consistent with a uniform participation of these lighter fragments in the radial expansion. Heavier fragments with $Z_f \geq 5$ do not follow this trend as clearly.

To further support these conclusions, energy spectra in the total CM frame at $\theta_{CM} = 90°$ are shown in Fig. 4 for Z_f = 2-6. The total fit and the contribution from participant source only are represented by the solid and dashed lines, respectively. Assuming a temperature T_1 = 15 MeV, the mean radial collective energy was estimated

by integrating these spectra and assuming $\langle E_r \rangle \approx \langle E \rangle - \frac{3}{2}T_1$. The resulting values for $\langle E_r \rangle$, are shown as open squares in the right panel of Fig.3; they are consistent with those obtained from the fits. Both results suggest that heavier fragments may not participate as fully in the collective expansion as lighter fragment. Such an effect could arise if heavier fragments originated from the more dense central regions of the expanding system.

In summary, energy spectra for IMF's produced in central Au+Au collisions at E/A = 100 MeV indicate a radial collective expansion at breakup. Values ranging from E_r/A = 8.3-12.5 MeV, extracted for the radial expansion energy decrease somewhat with the fragment charge, but they are relatively insensitive to assumptions about the density of the system at breakup, contributions from transverse flow or from the breakup of projectile and target spectator matter. The values for the collective energy of expansion are large, nearly one third to one half of the incident kinetic energy per nucleon in the CM frame, emphasizing the importance of this new aspect of collective flow and suggesting that expansion may, indeed, play a critical role in the large fragment multiplicities observed.

This work is supported by the National Science Foundation under Grant No. PHY-90-15255 and PHY-92-14992, and the U.S. Department of Energy under Contract No. DE-FG02-87ER-40316. W.G. Lynch and L.G. Sobotka acknowledge partial financial support from U.S. Presidential Young Investigator programs. CKG acknowledges partial support from Humboldt Research program. J.P. acknowledges the support of the DFG under Contract Po 256/2-1. We gracefully acknowledge the support and hospitality extended to us during our experiment at GSI.

References

1. M.B. Tsang et al., Phys. Rev. Lett. **71**, 1502 (1993).
2. G.F. Peaslee et al., Phys. Rev. **C49**, in press.
3. D.H.E. Gross et al., Phys. Rev. Lett. **56**, 1544 (1986).
4. J.P. Bondorf et al., Nucl. Phys. **A444**, 460 (1986).
5. W.A. Friedman, Phys. Rev. **C42**, 667 (1990).
6. J.E. Finn et al., Phys. Rev. Lett. **49**, 1321 (1982).
7. P.J. Siemens, Nature **305**, 410 (1983).
8. G. Peilert et al., Phys. Rev. **C39**, 1402 (1989); G. Peilert et al., Phys. Rev. **C46**, 1457 (1992).
9. D.H. Boal and J.N. Glosli, Phys. Rev. **C38**, 1870 (1988).
10. S.G. Jeong et al, report GSI-93-28.
11. H.W. Barz et al., Nucl. Phys. **A531**, 453 (1991).
12. W.Bauer et al., Phys. Rev. **C47**, 1838 (1993).
13. R.T. de Souza et al., Phys. Lett. **B300**, 29 (1993).
14. H.H. Gutbrod, A.M. Poskanzer, and H.G. Ritter, Rep. Prog. Phys. **52**, 1267 (1989)
15. H.H. Gutbrod, et al., Phys. Lett. **B 216**, 267 (1989); H.H. Gutbrod et al. Phys. Rev. **C42**, 640 (1990).
16. Y. Leifels et al., Phys. Rev. Lett. **71**, 963 (1993).
17. G.D. Westfall et al., Phys. Rev. Lett. **71**, 1986 (1993). Systematics in this paper suggest a "balance energy" below E/A = 70 MeV for the Au +Au system.
18. Q. Pan and P. Danielewicz, Phys. Rev. Lett. **70**, 2062 (1993)
19. R.T. de Souza et al., Nucl. Inst. Meth. **A 295**, 109 (1990). The Miniwall, a granular extension of the Miniball to forward scattering angles, uses technologies developed for the Dwarf Wall/Ball.
20. C. Schwarz et al., NSCL Annual Report (1994).
21. C. Cavata et al., Phys. Rev. **C42**, 1760 (1990).
22. Y.D. Kim et al., Phys. Rev. **C45**, 338 (1992).
23. J.P Bondorf et al., Nucl. Phys. **A333**, 285 (1980).

24. L. Phair et al., Nucl. Phys. **A548**, 489 (1992).

25. R. Trockel, Prog. Part. Nucl. Phys. **15**, 225 (1985).

26. L.D. Landau and E.M. Lifshitz, Statistical Physics 3^{d} Edition Part 1, Pergammon Press (1980).

27. Azimuthal averaging can be neglected for the participant source (i=1) because its source velocity is directed along the beam and in special cases for the spectator sources (i=2,3) when one is dealing with triple differential cross sections where the azimuthal orientation of the reaction plane is known.

28. W.C. Hsi, to be published.

29. W.K. Wilson et al., Phys. Rev. **C45**, 738 (1992).

30. M.B. Tsang et al., Phys. Rev. **C47**, 2717 (1993).

Table 1. Parameters for three source fits. (Note: Fits 1 and 2 are without and with expansion, respectively, and the units for a_i , T_i and V_i are ($MeV^{-2.5} \cdot sr^{-1}$), MeV, and MeV, respectively.)

Fit	Source	a_i	T_i	$v_{x,i}/c$	$v_{z,i}/c$	V_i	β_{exp}
1	1	9.2×10^{-11}	73.	0	0	35.	0
	2	3.2×10^{-11}	49.5	0.02	0.1	13.	0
2	1	1.1×10^{-9}	13.	0	0	0	0.16
	2	3.7×10^{-11}	59.	0.02	0.1	13.	0

Figure Captions

Fig. 1: Comparisons of the energy spectra for Boron fragments emitted to Θ_{lab}=28°, 35.5°, 45°, 57.5°, 72.5°, 90° and 110° (solid points) with corresponding moving source fits. Upper Panel: The solid lines correspond to fits obtained with Eq.1 and no radial expansion. Lower panel: The solid lines correspond to fits obtained with Eqs. 1 and 4, incorporating a radial expansion. The dashed lines in both panels correspond to the respective contributions from the participant sources alone.

Fig. 2: The open squares correspond to measured α-α correlations obtained for central collisions at E/A=400 MeV and $0.25 \leq y_\alpha/y_{beam} \leq 0.5$. The open circles correspond to the corresponding α-α correlations for central collisions at E/A=100 MeV. The solid circles correspond to α-α correlations for central collisions at E/A=100 MeV and $-0.25 \leq y_\alpha/y_{beam} \leq 0.25$.

Fig. 3: Left Panel: The open points correspond to best fit values for the radial expansion velocities as a function of the fragment charge. The solid points are the corresponding values obtained when T_1 is constrained to be 15 MeV. Right Panel: The solid points depict the dependence of the mean radial collective energy $\langle E_r \rangle$ extracted from the fits upon the fragment charge. The open points depict the corresponding values extracted from Fig. 4 assuming T_1 = 15 MeV. Both values are plotted at the mass of the most abundant stable isotope.

Fig. 4: Energy spectra in the CM frame for various fragments detected at $\theta_{CM} = 90° \pm 10°$. The solid lines corresponds to the three source fit assuming a radial expansion. The dashed lines depict the participant source alone.

MSU-094-038

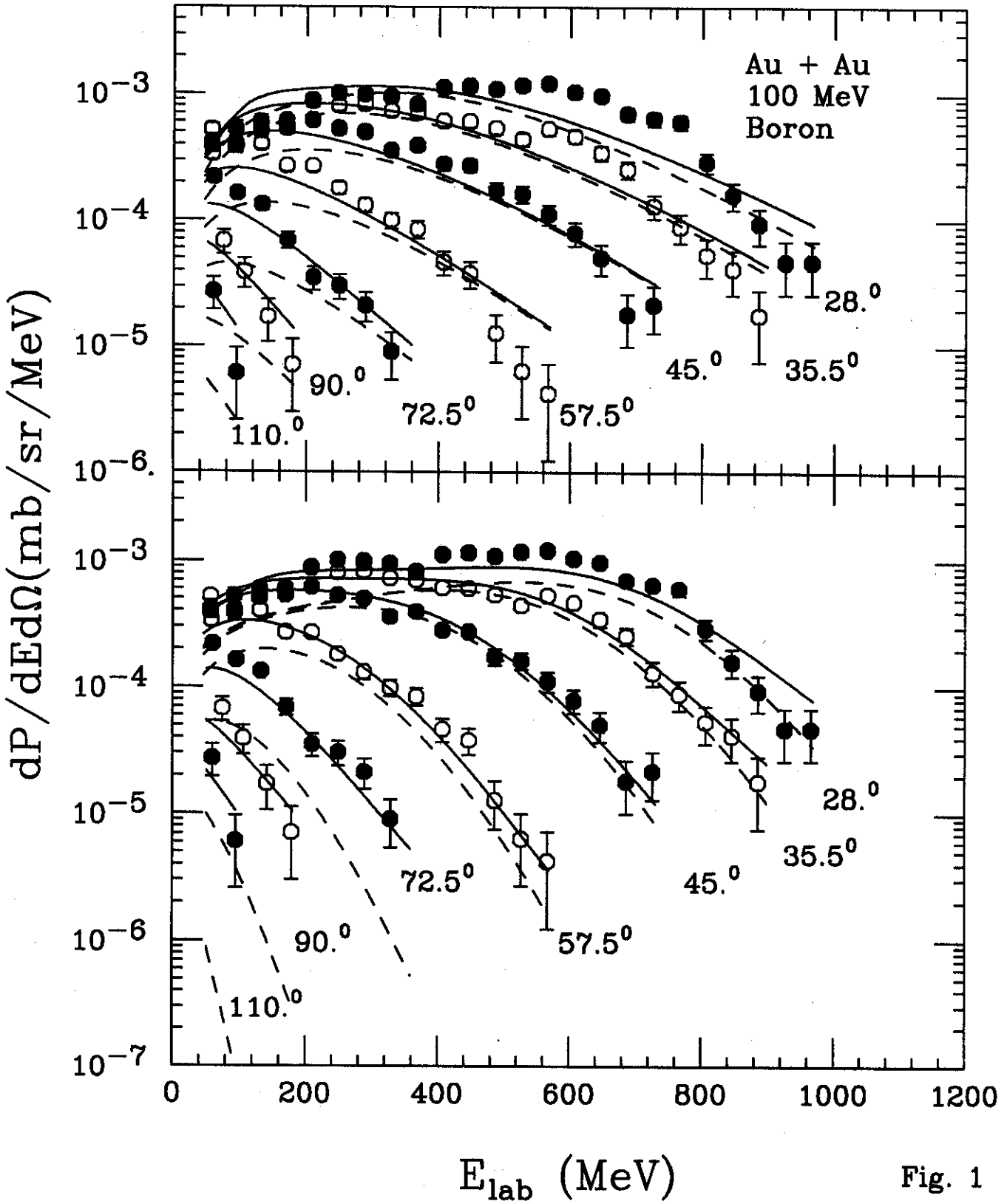

Fig. 1

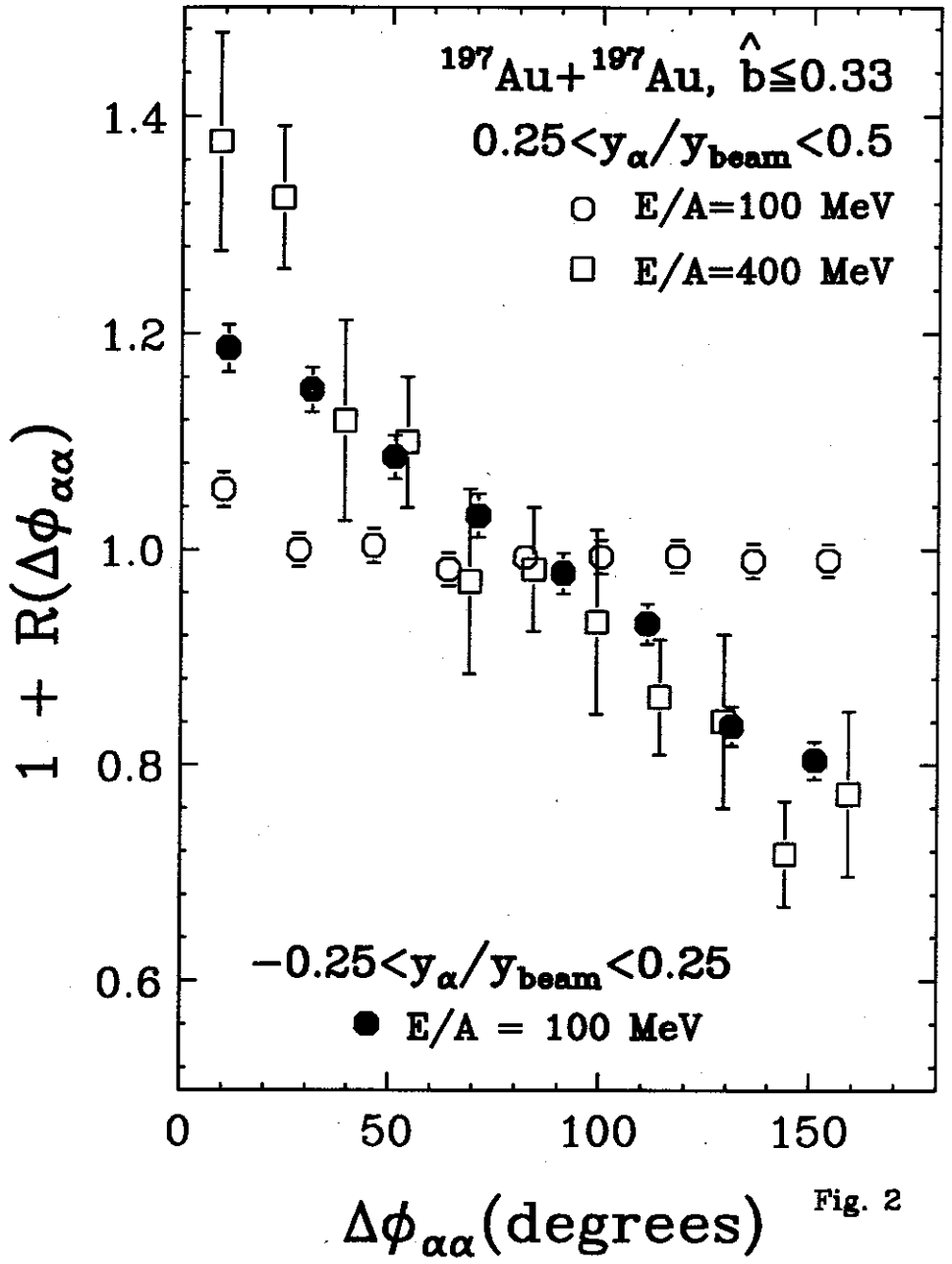
^{197}Au+^{197}Au, $\hat{b}\leq 0.33$
$0.25<y_\alpha/y_{beam}<0.5$
E/A=100 MeV
E/A=400 MeV
$-0.25<y_\alpha/y_{beam}<0.25$
E/A = 100 MeV
$1 + R(\Delta\phi_{\alpha\alpha})$
$\Delta\phi_{\alpha\alpha}$(degrees)
0.6
0.8
1.0
1.2
1.4
0
50
100
150

Fig. 2

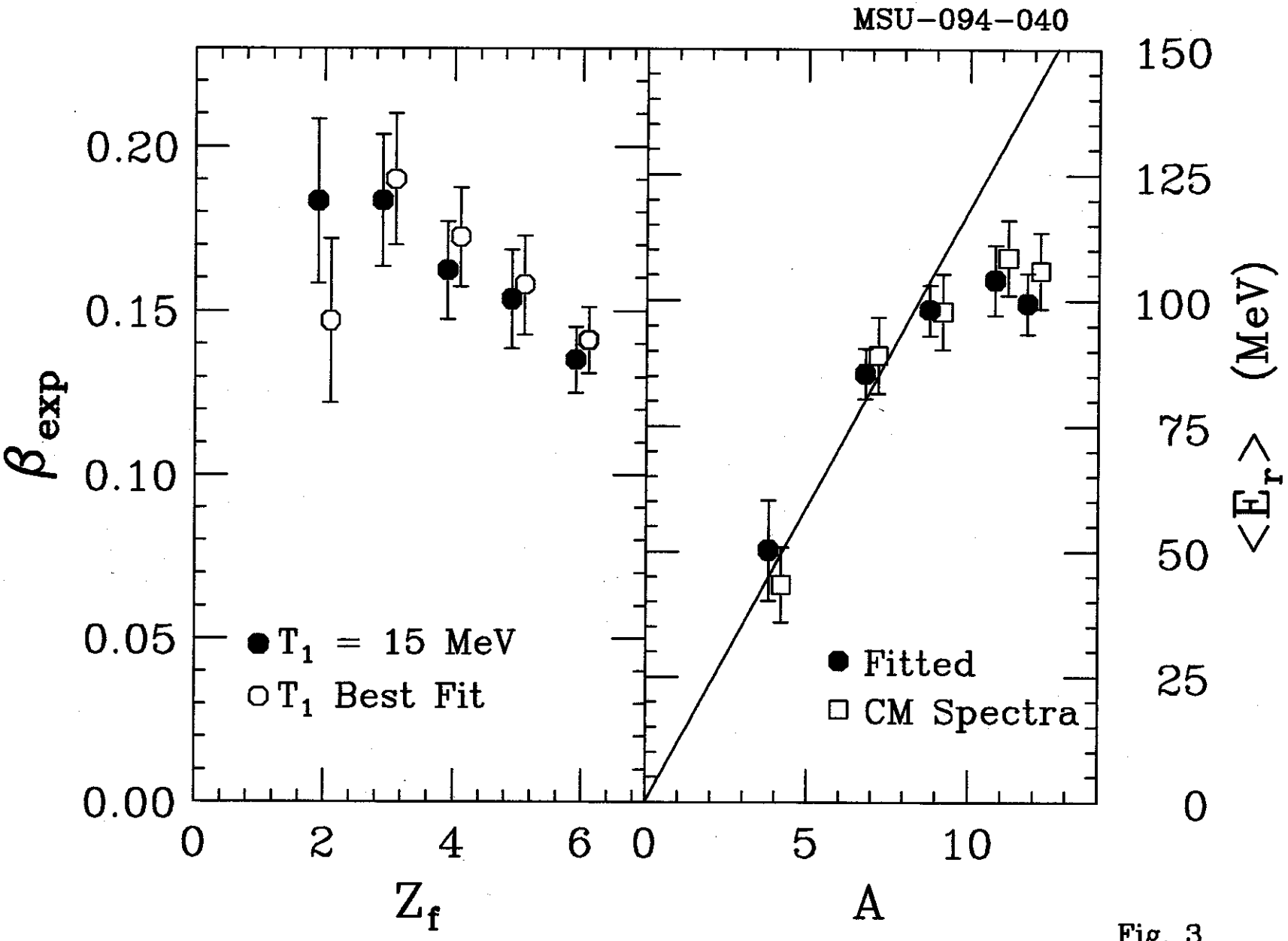
MSU-094-040
0.20
0.15
0.10
0.05
0.00
β_{exp}
0
2
4
6
Z_f
T_1 = 15 MeV
T_1 Best Fit
0
5
10
A
Fitted
CM Spectra
150
125
100
75
50
25
0
$<E_r>$ (MeV)

Fig. 3

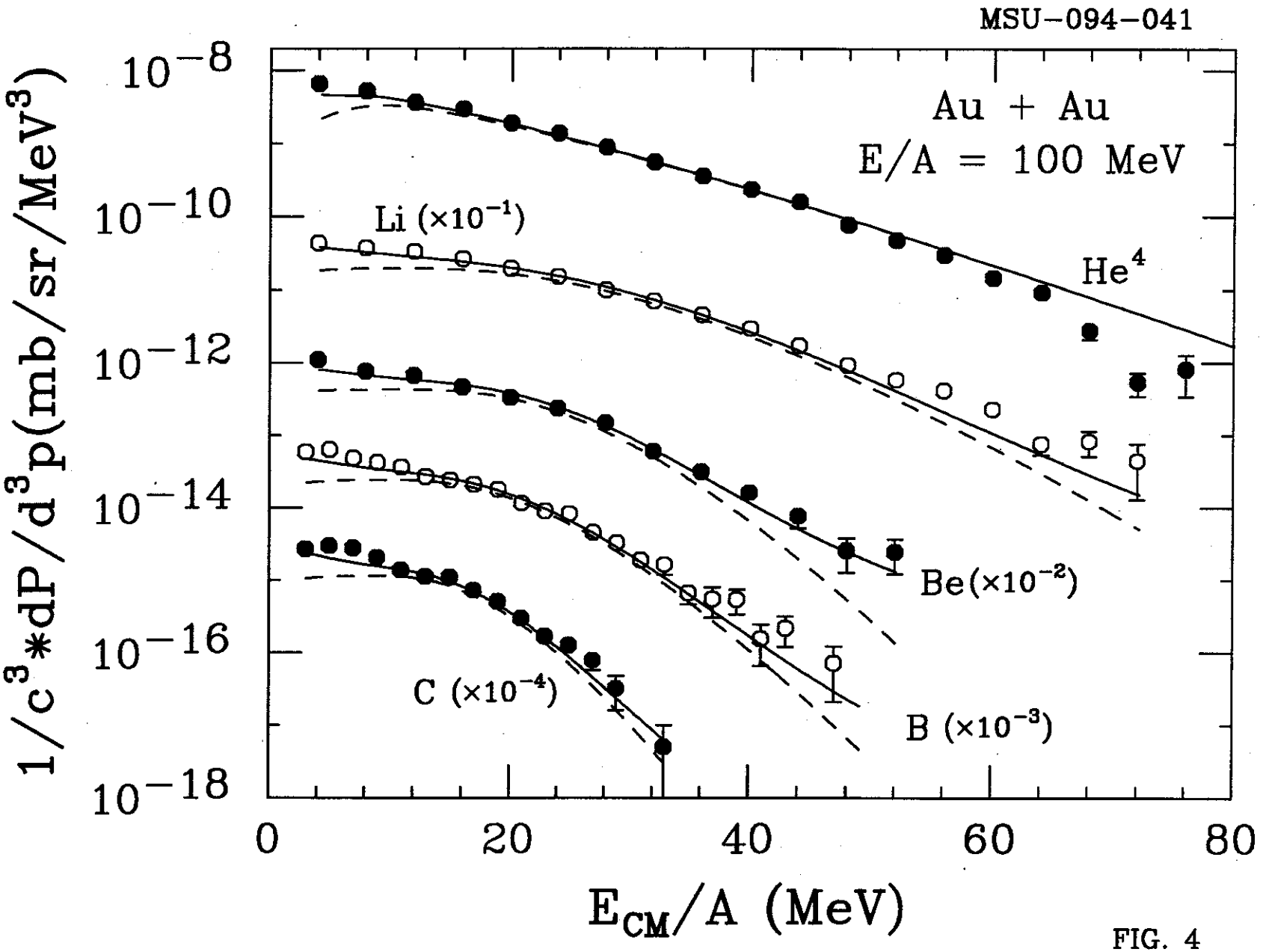
MSU-094-041
Au + Au
E/A = 100 MeV
Li (×10⁻¹)
He⁴
Be(×10⁻²)
B (×10⁻³)
C (×10⁻⁴)
1/c³*dP/d³p(mb/sr/MeV³)
E_CM/A (MeV)
10⁻⁸
10⁻¹⁰
10⁻¹²
10⁻¹⁴
10⁻¹⁶
10⁻¹⁸
0
20
40
60
80

FIG. 4